

Calibration of the TSI 3025 CPC – EMLACE2, DMIMS06, and NASA06

B.Pokharel and J.Snider

1 September 2006

Summary

In October 2004 the Department of Atmospheric Science purchased a TSI 3025 Ultrafine Condensation Particle Counter, hereafter referred to as the 3025 CPC. Calibration studies were conducted in the Keck Laboratory prior to and after the EMLACE2, DMIMS06, and NASA06 field experiments. These demonstrate two sources of measurement bias: 1) Concentrations reported by the 3025 CPC exceed those reported by two TSI 3010 CPCs by ~20%. This is evident in comparison studies done at relatively large test particle concentrations ($>100 \text{ cm}^{-3}$) and is thought due to a bias in the aerosol flow rate through the 3025 CPC. 2) For tests conducted at particle concentrations less than 100 cm^{-3} an offset bias is evident. This is attributed to an analog offset in the Keck Lab data acquisition system.

Introduction

Figure 1 shows that the 3025 CPC detects 2.5 nm (nanometer) particles with a 50% counting efficiency. This size is a factor of four smaller than the particle size corresponding to a 50% counting efficiency size in the 3010 CPC. Another advantage of the 3025 CPC is its 1 s response time; this is a factor of five smaller than the response time of the 3010 CPC (The response times is defined as the time required for the instrument to reach 95% of a stepped input concentration of particles substantially larger than the 50% counting efficiency size).

A disadvantage of the 3025 CPC, relative to the 3010 CPC, is that the flow stream entering the instrument is split into three streams: the sheath, bypass and aerosol streams (Figure 2). The value of the latter is used within the instrument for deriving concentration; a fixed value is assumed ($0.5 \text{ cm}^3 \text{ s}^{-1} = 30 \text{ cm}^3 \text{ min}^{-1}$). The aerosol flow in the 3025 CPC is calibrated by adjusting the sheath and total flow streams. Because these two flows are of comparable magnitude, 270 and $300 \text{ cm}^3 \text{ min}^{-1}$ respectively, error in their calibration can lead to bias in the aerosol flow rate and thus to bias in the derived aerosol concentration. Hence, concentrations reported by a 3025 CPC are not expected to be as accurate as those reported by the 3010 CPC. For the latter the flow stream entering the instrument is not split and its value is $1000 \text{ cm}^3 \text{ min}^{-1}$ ($17 \text{ cm}^3 \text{ s}^{-1}$), i.e., 34 times the aerosol flow in the 3025 CPC.

Here we discuss laboratory measurements reported by the 3025 and 3010 CPCs. Test aerosols were composed of either ammonium sulfate or polystyrene latex (PSL) particles. The test aerosols were mobility-classified in differential mobility analyzer (DMA) prior to sampling by the CPCs. The experimental setup is shown in Figure 3a (20050910 and 20050911), Figure 3b (20060211), Figure 3c (20060328), and Figure 3d (20060706,

20060707, 20060708 and 20060709). Table 1 summarizes the data file names, netcdf variable names and the Keck data system input channels.

Results -

Figures 4a, 4b and 4c present comparisons of concentrations measured by the 3025 CPC and the two 3010 CPCs (CPC-1 and CPC-3). The data points are 316 s averages of the CPC concentration measurements. The length of the averaging interval is dictated by the time required for measurement of the size distribution with the SMPS-A. In these figures only data corresponding to the test aerosols with mode diameters larger than 30 nm are shown. Results can be summarized by the following 3025 CPC correction equations

$$[CN]_1 = 16(\pm 4) + 0.82(\pm 0.01) \cdot [CN]_{3025} \quad (\text{analog input 25}) \quad (1)$$

$$[CN]_1 = 26(\pm 7) + 0.83(\pm 0.01) \cdot [CN]_{3025} \quad (\text{analog input 22}) \quad (2)$$

$$[CN]_3 = 16(\pm 2) + 0.81(\pm 0.01) \cdot [CN]_{3025} \quad (\text{analog input 22}) \quad (3)$$

We define $[CN]_1$ as the corrected 3025 CPC concentration measurement. This is derived as a linear regression of the 3010 CPC-1 and the uncorrected 3025 CPC data (Figures 4a and 4b). Similarly, $[CN]_3$ is defined as the corrected 3025 CPC concentration based on 3010 CPC-3 and uncorrected 3025 CPC data (Figure 4c). Departure of the slope of the correction equations from unity is attributed to a positive departure between the actual and the nominal aerosol flow rate through the 3025 CPC. Other explanations for the bias, i.e., bias in the determination of the aerosol flow rate through the 3010 CPC have been eliminated by measurement of the aerosol flow into that instrument. Another plausible explanation, counting efficiency, was eliminated by only considering data from experiments with test particle diameters larger than 30 nm.

Evidence for an analog offset introduced in the data acquisition system is presented in Figure 5. During this experiment (20060328, 20060706, 20060707, 20060708 and 20060709) we recorded both the analog and pulsed outputs of the 3025 CPC (middle and bottom panels). Clear indication of the offset is evident between 11:00 and 11:14 where the analog 3025 CPC signal plots at -12 cm^{-3} and the 3010 CPC-3 is indicating $+4 \text{ cm}^{-3}$. Averages of the output from the analog 3025 CPC channel are reported in the fifth column of Table 2. Also shown (sixth column of Table 2) are concentrations derived as

$$[CN]_3 = \frac{\bar{P} \cdot 0.81}{0.5} \quad (4)$$

where \bar{P} is the 316 s average of the output from the pulsed 3025 CPC channel and the numerical constants are defined by the slope of Equation 3 and the nominal aerosol flow rate ($0.5 \text{ cm}^3 \text{ s}^{-1}$).

This analysis was repeated for data collected with the 3010 CPC-1 and the 3025 CPC; results are shown in Tables 3a, 3b, 3c and 3d. Data was collected on 20060706, 20060707, 20060708 and 20060709, respectively.

$$[CN]_1 = \frac{\bar{P} \cdot 0.83}{0.5} \quad (5)$$

Here the numerical constant in the numerator is defined by the slope of Equation 2.

The seventh columns of Tables 2, 3a, 3b, 3c and 3d are percentage differences among values derived from Equations 4 and 3 (Table 2) or from Equations 5 and 2 (Tables 3a, 3b, 3c and 3d). The good agreement indicates that the slope in Equations 2 and 3 results from bias in the 3025 flow calibration. Further, the agreement also indicates that the intercept in Equations 2 and 3 results from an analog offset generated in the Keck data system.

Conclusions –

Measurements from three CPCs (the 3025, 3010-1 and 3010-3) reveal bias in concentration measurements reported by the 3025 CPC. Correction equations for the 3025 CPC are presented. Two biases are uncovered. The first is apparent over a broad range of concentration and the other is only evident at low concentrations. For the first we speculate that the true value of the aerosol flow rate through the 3025 CPC is ~20% larger than the nominal value. This conjecture is supported by laboratory data showing that an aerosol flow rate correction applied to pulsed outputs from the 3025 CPC (i.e., Equation 4 and Equation 5 and the sixth column of Table 2 and Table 3) produce concentration values consistent the reference 3010 CPC. The second bias is only evident at particle concentrations less than 100 cm⁻³ and appears to originate from an offset introduced in the Keck Lab data acquisition system.

Recommendations –

- 1) Accurate and precise flow measurement capability is needed for inline measurements made at volumetric flow rates ~ 300 cm³ min⁻¹. Relative absolute error (bias and precision) associated with these flow measurements should be less than 5%.
- 2) The data system offset can be estimated by sampling filtered air with the 3025 CPC. These tests should be conducted for several tens of seconds so that a robust statistical description of the average bias and its standard deviation can be evaluated.

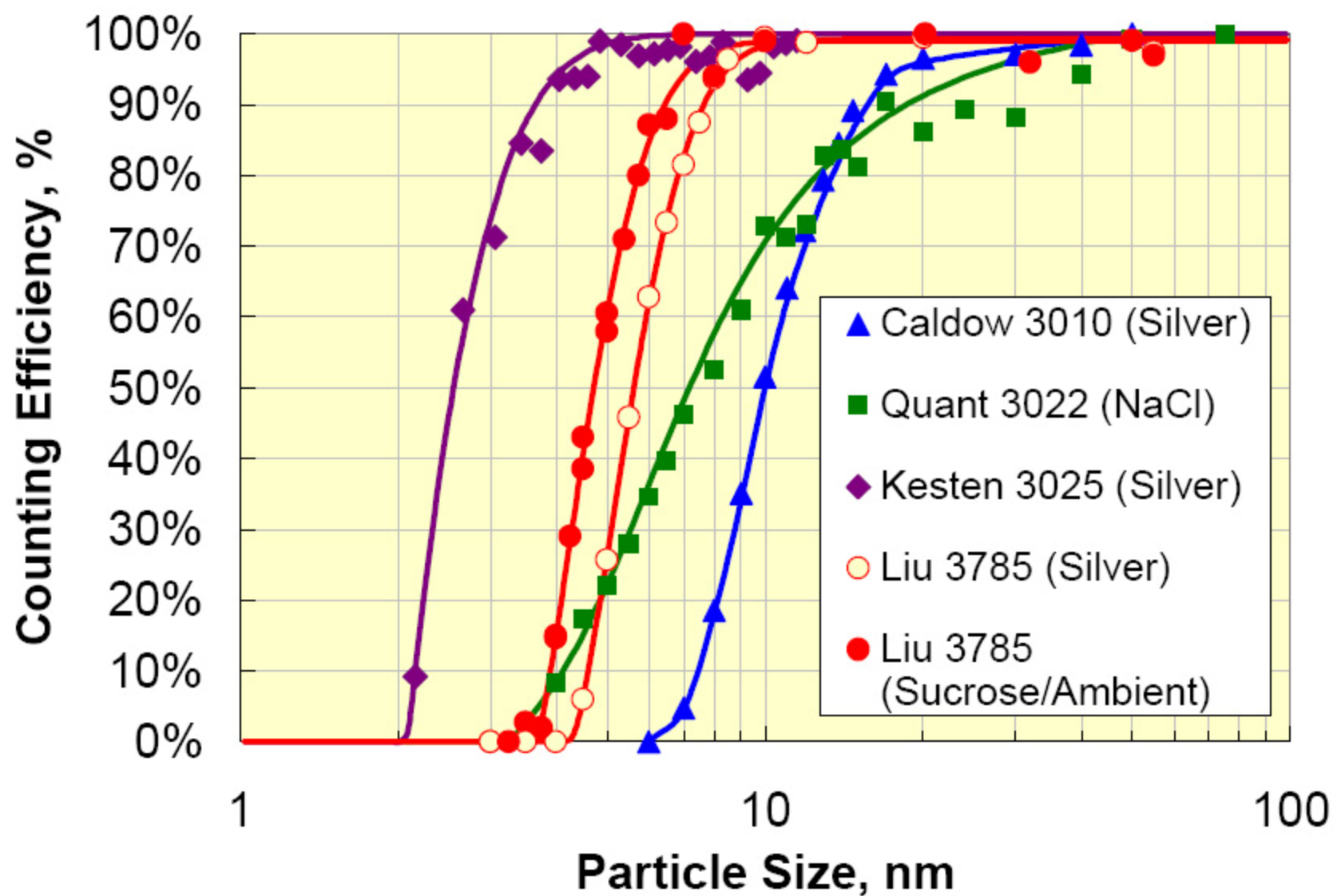


Figure 1 – Counting efficiencies of different condensation particle counters

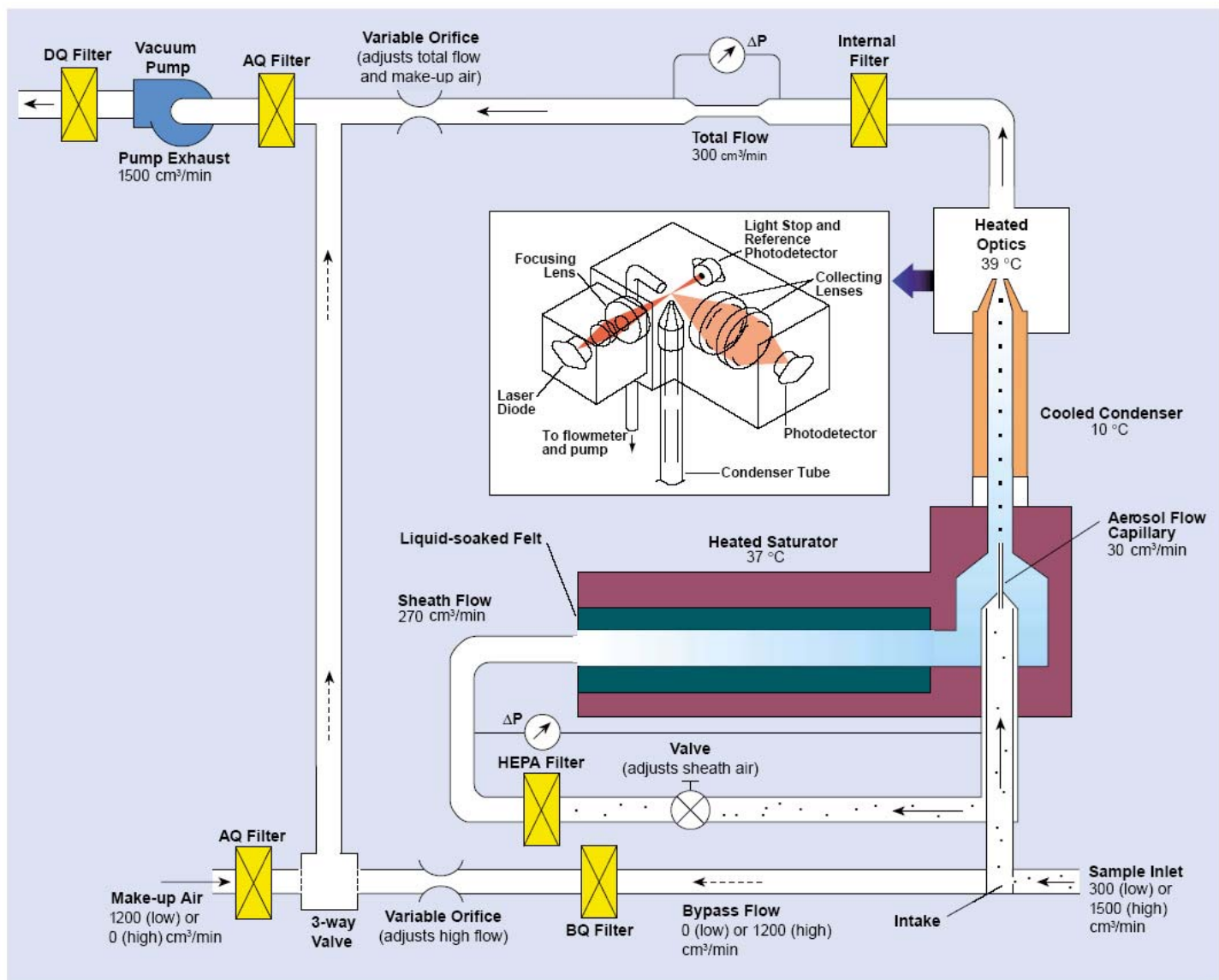


Figure 2 - Flow schematic of the 3025 CPC.

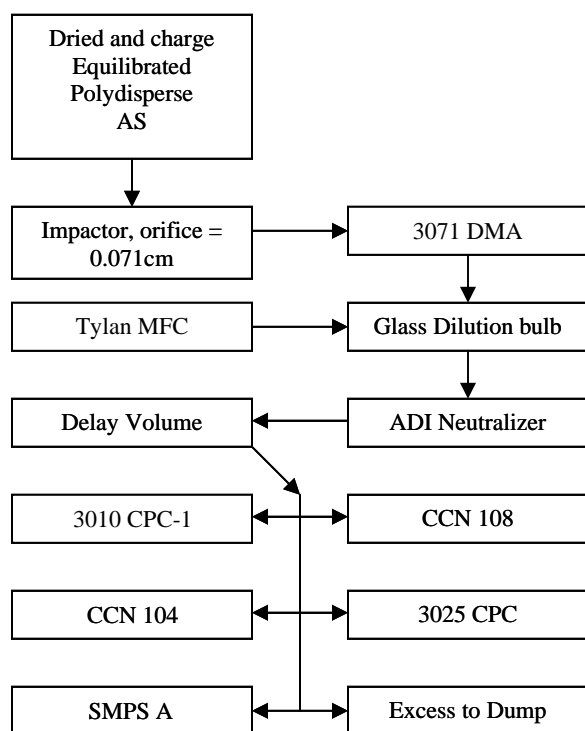


Figure 3a – Schematic of the lab setup on 20050910 and 20050911

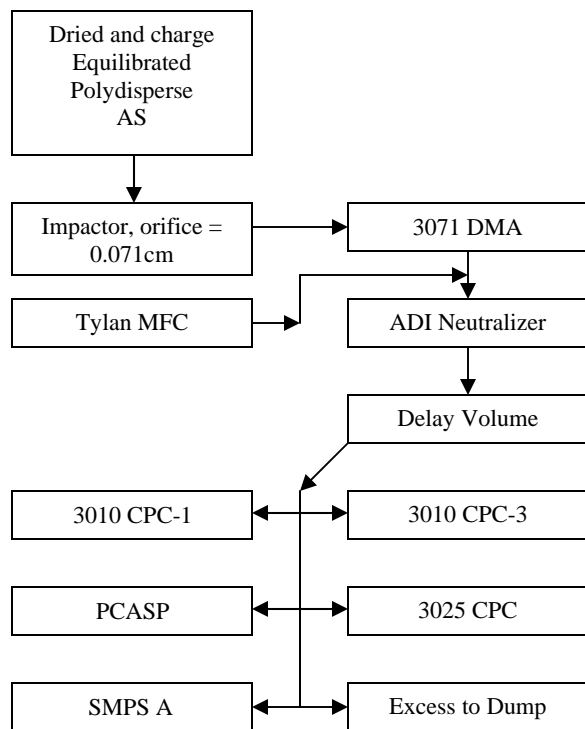


Figure 3b – Schematic of the lab setup on 20060211

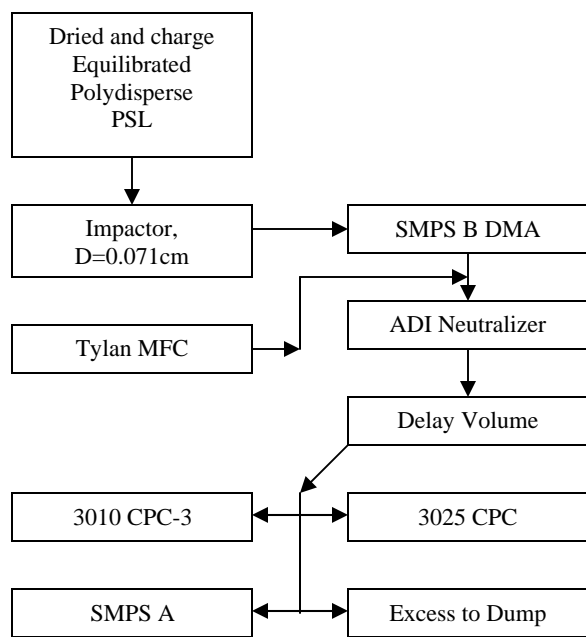


Figure 3c - Schematic of the lab setup on 20060328

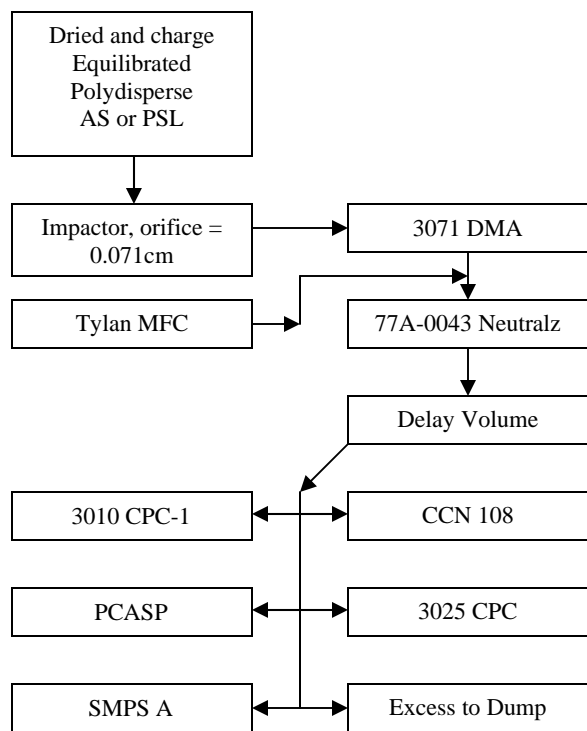


Figure 3d - Schematic of the lab setup on 20060706, 20060707, 20060708 and 20060709

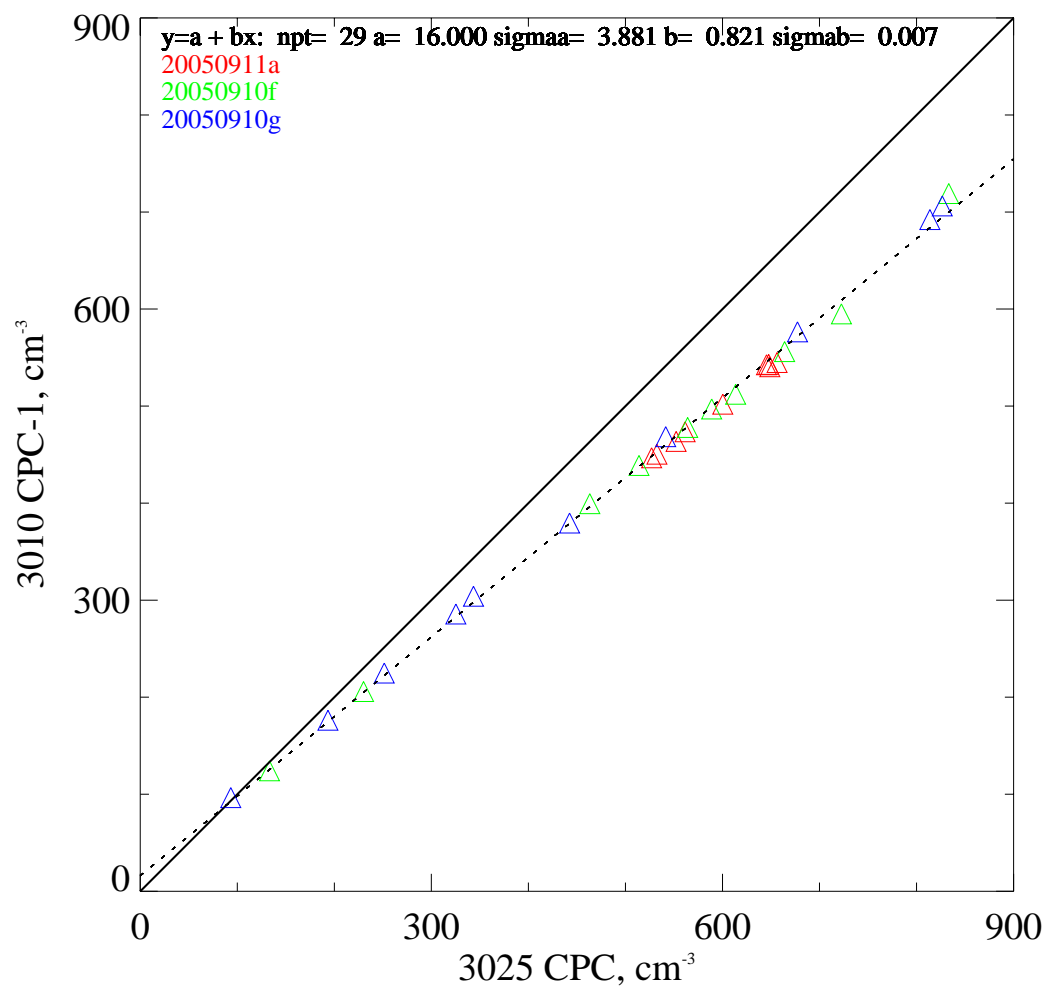


Figure 4a - Plot of concentration measured by the 3025 CPC versus the 3010 CPC-1 on 20050910 and 20050911 for the mode diameter larger than 30 nm. The solid line is the 1:1 line and dashed line is fitting line for $y = a + bx$.

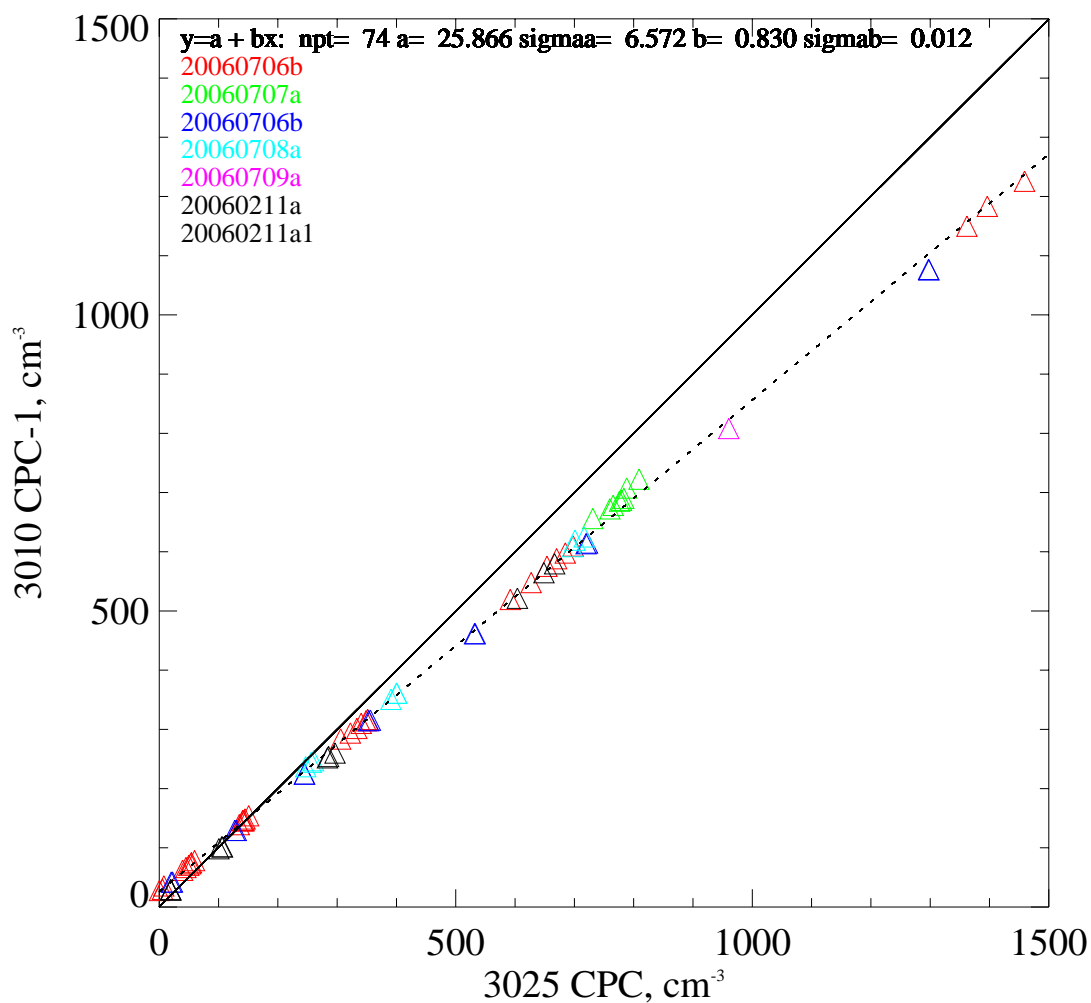


Figure 4b - Plot of concentration measured by the 3025 CPC versus the 3010 CPC-1 on 20060211, 20060706, 20060707, 20060708 and 20060709 for the mode diameter larger than 30 nm. The solid line is the 1:1 line and dashed line is fitting line for $y = a + bx$.

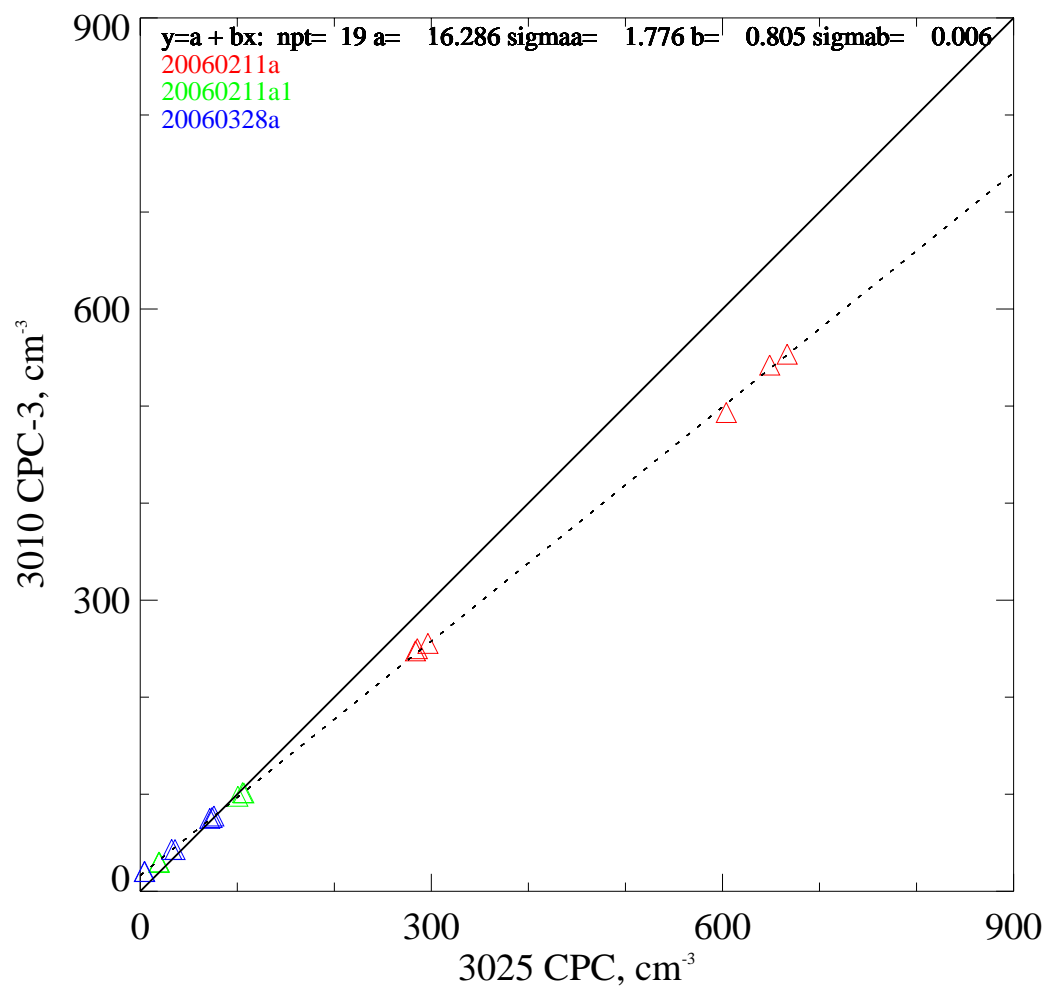


Figure 4c - Plot of concentration measured by the 3025 CPC versus the 3010 CPC-3 on 20060211 and 20060328 for the mode diameter larger than 30 nm. The solid line is the 1:1 line and dashed line is fitting line for $y = a + bx$.

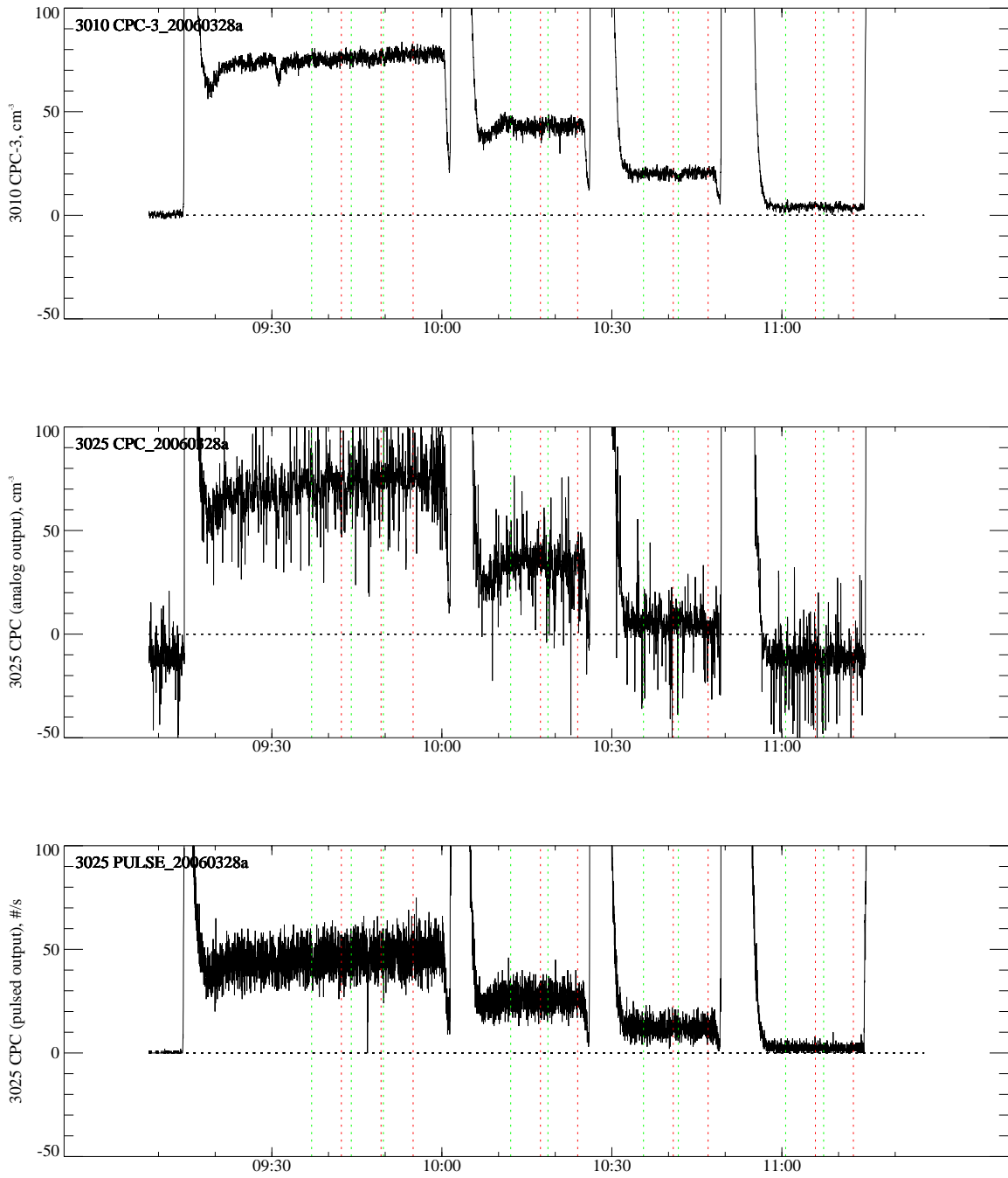


Figure 5 - Time series (1 Hz sampling) of CPC signals on 20060328. Green and red vertical lines indicate the start and stop times of the SMPS-A scan intervals. Top) 3010 CPC analog output, Middle) 3025 CPC analog output, and Bottom) 3025 CPC pulsed output.

Table 1- Data Files, netcdf variable names and analog input channels

netcdf file name	smgs file name	variablename 3010 CPC	variablename 3010 CPC	variablename 3025 CPC	Analog Input for 3025 CPC	variablename for 3025 CPC
20050910b.c1.nc	sep105f.txt	cpc1_aconc		UFN_RAW	25	
20050911a.c1.nc	sep115a.txt	cpc1_aconc		UFN_RAW	25	
20050910c.c1.nc	sep105g.txt	cpc1_aconc		UFN_RAW	25	
20060211b.c1.nc	feb1106a.txt	CPC1_CONC_RAW	CPC3_CONC_RAW	UFN_RAW	22	
20060211c.c1.nc	feb1106a.txt	CPC1_CONC_RAW	CPC3_CONC_RAW	UFN_RAW	22	
20060328a.c1.nc	mar2806a.txt		CPC3_CONC_RAW	UFN_RAW	22	UFN_Pulse
20060706a.c1.nc	jul0606a.txt	CPC1_CONC_RAW		UFN_RAW	22	UFN_Pulse
20060706b.c1.nc	jul0606b.txt	CPC1_CONC_RAW		UFN_RAW	22	UFN_Pulse
20060707a.c1.nc	jul0607a.txt	CPC1_CONC_RAW		UFN_RAW	22	UFN_Pulse
20060707b.c1.nc	jul0607a.txt	CPC1_CONC_RAW		UFN_RAW	22	UFN_Pulse
20060708a.c1.nc	jul0608a.txt	CPC1_CONC_RAW		UFN_RAW	22	UFN_Pulse
20060709a.c1.nc	jul0609a.txt	CPC1_CONC_RAW		UFN_RAW	22	UFN_Pulse

Table 2 - Correction of the 3025 CPC concentration in Equations 3 and 4

Local Time	SMPS-A Mode Diameter	3010-3 CPC Conc. (analog output)	3025 CPC Conc.	Corrected 3025 CPC Conc. (Eq. 3)	Pulse CPC 3025 Conc. (Eq. 4)	Percent Difference $100 \times (\text{Eq. 3} - \text{Eq. 4}) / \text{Eq. 4}$
hhmmss	nm	cm ⁻³	cm ⁻³	cm ⁻³	cm ⁻³	%
9:37:01	496	75	72	74	74	1
9:44:01	496	76	74	76	74	2
9:49:41	496	78	76	77	76	2
10:12:09	496	43	36	45	43	6
10:18:43	496	43	32	42	43	-1
10:35:35	496	20	4	19	20	-1
10:41:44	496	21	5	20	20	0
11:00:40	533	4	-12	6	4	49
11:07:22	496	4	-12	6	3	82

Table 3(a) - Correction of the 3025 CPC concentration in Equations 2 and 5 for 20060706

Local Time	SMPS-A Mode Diameter	3010-1 CPC Conc. (analog output)	3025 CPC Conc.	Corrected 3025 CPC Conc. (Eq. 2)	Pulse CPC 3025 Conc. (Eq. 5)	Percent Difference $100 \times (\text{Eq. 2} - \text{Eq. 5}) / \text{Eq. 5}$
hhmmss	nm	cm-3	cm-3	cm-3	cm-3	%
10:00:38	31	42	22	44	46	-3
10:06:40	31	42	20	43	46	-6
10:22:05	31	130	127	132	135	-3
10:27:31	31	129	130	134	135	-1
10:37:56	31	225	245	229	232	-1
10:46:58	31	224	245	229	231	-1
10:57:06	31	315	353	319	322	-1
11:03:09	31	316	356	321	323	0
11:12:29	31	462	532	467	471	-1
11:17:57	31	462	533	468	472	-1
11:26:26	31	614	720	623	625	0
11:34:02	31	615	722	625	628	0
11:44:29	31	1077	1297	1103	1102	0
11:50:11	31	1076	1298	1103	1103	0
12:53:48	188	1226	1459	1237	1237	0
13:06:39	188	548	627	547	550	-1
13:11:48	188	519	592	517	519	0
13:20:08	188	315	349	316	319	-1
13:27:08	188	302	333	303	305	-1
13:40:16	188	146	141	143	147	-3
13:45:23	188	139	135	138	141	-2
13:56:37	195	62	39	59	65	-10
14:06:19	188	73	53	70	75	-7
14:24:09	195	30	5	31	34	-9
14:31:34	188	28	0	26	31	-16
14:49:51	188	26	-3	24	29	-20
15:02:01	188	78	60	75	80	-6
15:14:20	188	145	141	143	146	-2
15:26:02	188	294	322	293	295	-1
15:36:16	188	610	698	605	608	0
15:50:56	188	1183	1396	1185	1185	0
16:04:12	188	1150	1362	1156	1157	0
16:18:23	188	598	685	594	596	0
16:30:28	188	310	341	309	312	-1
16:41:03	188	146	143	145	148	-2
16:50:33	188	67	45	63	68	-7
16:59:55	188	26	-1	25	29	-15

17:11:20	188	36	8	32	38	-14
17:19:44	188	71	50	67	73	-7
17:29:52	188	154	151	151	155	-3
17:43:26	188	317	351	318	320	-1
17:52:10	188	575	654	569	573	-1
18:01:28	188	588	670	582	586	-1
18:14:42	188	284	306	280	282	-1
18:22:30	188	149	145	146	149	-2
18:33:09	188	75	54	71	76	-7
18:41:38	188	28	0	26	31	-17

Table 3(b) - Correction of the 3025 CPC concentration in Equations 2 and 5 for 20060707

Local Time	SMPS-A Mode Diameter	3010-1 CPC Conc. (analog output)	3025 CPC Conc.	Corrected 3025 CPC Conc. (Eq. 2)	Pulse CPC 3025 Conc. (Eq. 5)	Percent Difference $100 \times (\text{Eq. 2} - \text{Eq. 5}) / \text{Eq. 5}$
hhmmss	nm	cm-3	cm-3	cm-3	cm-3	%
12:07:23	113	614	892	766	767	0
12:19:06	113	559	892	766	767	0
12:25:37	113	329	887	762	765	0
13:27:57	76	690	783	676	677	0
13:58:21	76	687	780	673	675	0
14:05:33	76	686	776	670	672	0
14:23:04	76	678	765	661	662	0
14:39:24	76	673	760	657	657	0
15:31:40	51	656	731	633	635	0
15:49:10	36	708	788	680	683	0
15:59:29	36	723	809	697	699	0

Table 3(c) - Correction of the 3025 CPC concentration in Equations 2 and 5 for 20060708

Local Time	SMPS-A Mode Diameter	3010-1 CPC Conc. (analog output)	3025 CPC Conc.	Corrected 3025 CPC Conc. (Eq. 2)	Pulse CPC 3025 Conc. (Eq. 5)	Percent Difference $100 \cdot (\text{Eq. 2} - \text{Eq. 5}) / \text{Eq. 5}$
hhmmss	nm	cm-3	cm-3	cm-3	cm-3	%
16:01:41	496	237	247	231	232	0
16:09:07	496	247	260	242	243	0
16:17:19	496	245	256	239	241	-1
16:57:57	202	351	391	350	351	0
17:03:32	202	361	401	359	359	0
17:09:44	202	361	400	358	359	0
17:35:55	126	609	697	604	605	0
17:41:21	126	620	701	608	610	0
17:47:33	126	625	717	621	622	0

Table 3(d) - Correction of the 3025 CPC concentration in Equations 2 and 5 for 20060709

Local Time	SMPS-A Mode Diameter	3010-1 CPC Conc. (analog output)	3025 CPC Conc.	Corrected 3025 CPC Conc. (Eq. 2)	Pulse CPC 3025 Conc. (Eq. 5)	Percent Difference $100 \cdot (\text{Eq. 2} - \text{Eq. 5}) / \text{Eq. 5}$
hhmmss	nm	cm-3	cm-3	cm-3	cm-3	%
10:16:48	17	61	168	166	166	0
10:25:02	22	425	674	586	584	0
10:35:20	27	740	959	822	824	0
10:44:57	32	808	960	823	821	0
11:03:57	31	800	996	852	852	0
11:09:55	27	543	723	626	624	0
11:17:32	22	382	640	557	558	0
11:25:30	17	56	181	176	176	0